Chapter 4. Evaporation and discharge dynamics of highly charged droplets of heptane, octane, and *p*-xylene generated by electrospray ionization

Adapted from Grimm, Ronald L. and Beauchamp, J. L. *Anal. Chem*. **2002**, *74*, 6291.

4.1. Abstract

We report studies of the evaporation and discharge dynamics of highly charged droplets generated by electrospray ionization from *n*-heptane, *n*-octane, and *p*-xylene doped with Stadis-450, a conductivity enhancing agent. A phase Doppler anemometer (PDA) characterizes individual droplets moving through the uniform electric field within an ion mobility cell according to size, velocity, and charge. Repeated reversal of the electric field allows multiple PDA measurements on selected droplets with diameters ranging from 3 to 60 μm and up to 10^7 elementary positive charges. This "ping-pong" technique provides individual droplet histories from which we determine the dynamics of solvent evaporation and charge loss. On average, *n*-heptane discharges at 101% of the Rayleigh limit of charge, while *n*-octane and *p*-xylene droplets discharge at 87% and 89% of their respective limits. Discharge events release an average of 19% of the charge in *n*-heptane, and 17% of the charge in both *n*-octane and *p*-xylene. Within the limits of the measurements, no detectable change in droplet diameter accompanies observed discharge events, indicating the loss of a relatively small fraction of the total volume. We compare these results to previous experiments, theoretical models for droplet evaporation and discharge, and predictions from the Rayleigh model. We report both Stadis-450 and

triethylamine mass spectra in octane, and discuss issues regarding the use of hydrocarbon solvents in electrospray mass spectrometry.

4.2. Introduction

Polar liquids are the primary solvents for electrospray ionization and their discharge dynamics have been well studied.[1] Lord Rayleigh developed the critical theories of charged droplets, balancing the forces of surface tension and charge repulsing to determine charged droplet stability. His work suggests that, in a droplet of radius r and surface tension σ in a medium of electric permittivity ε, charge repulsion will overcome surface tension at a charge q_R given by eq (4.1). When this condition is met, Rayleigh predicts that droplets undergo a disruptive event in which "the liquid is thrown out in fine jets, whose fineness, however, has a limit". Although this suggests a mechanism for the discharge event, his model lacks a quantitative description of the charge loss of specific relationships between progeny drop or droplets and the parent.[1]

$$q_R = 8\pi\varepsilon^{1/2}\sigma^{1/2}r^{3/2}$$
(4.1)

Recent studies in our laboratory focused on the more common electrospray solvents water, methanol, and acetonitrile. This work suggests a solvent dependence on the charge loss and the percent Rayleigh limit at discharge.[1,2] These results are summarized in Table 4.1.

On the other hand, high-volatility hydrocarbons and similar low-conductivity solvents are not widely employed for electrospray mass spectrometry and their Rayleigh discharge characteristics have received less attention than more commonly used polar solvents such as water and methanol. Several researchers present spectra of crude oils

and hydrocarbon fuels dissolved in solutions of polar solvents.[3-5] Rebek and coworkers report the use of benzene and xylene without the addition of polar solvents,[6,7] but few others routinely employ hydrocarbons as solvents for analytical applications of electrospray mass spectrometry. Tang and Gomez generated a stable electrospray of n-heptane, focusing on the dynamics of the spray itself,[8] as well as size determinations and percent Rayleigh limit approximations for droplets within the spray.[9] Most recently Leisner and coworkers have developed experimental methodologies for studying the evaporation and discharge dynamics of low-volatility solvents. They have acquired images of a discharge event from glycerol characterized by simultaneous, symmetrical emission of two fine streams of progeny droplets from opposite sides of the droplet.[10] This contrasts with the previous work of both Gomez and Tang,[9] as well as Kebarle and coworkers[11] who present visual evidence of droplet distortions leading to discharge from a single point on a parent droplet near the Rayleigh limit for heptane and methanol, respectively.

We report the evaporation and discharge dynamics of three volatile hydrocarbon solvents, and relate the dynamics to previously researched solvents widely employed in electrospray mass spectrometry. The present work investigates positively charged 3-60 μm droplets of *n*-heptane, *n*-octane, and *p*-xylene with up to 10^7 elementary charges. To reduce droplet sizes to a range accessible for measurement using our experimental methodology, Stadis-450, a conductivity enhancing agent, is added to each of these solvents. Previous studies demonstrated that Stadis-450 does not significantly affect the surface tension and the dielectric constant of bulk heptane in concentrations up to 3%.[8]

Discharges are characterized by measuring the droplet diameter and charge, as well as the charge loss at the time of the event. We are not able to detect mass loss associated with a discharge event. Overall mass loss due to evaporation is measured and compared against models discussed in chapter three. Table 4.1 lists the calculated solvent parameters, *s*, for the evaporation of acetonitrile, methanol, water, heptane, octane and *p*-xylene. We additionally present data illustrating the use of these hydrocarbon solvents in conventional electrospray mass spectrometry analyses. Spectra are reported for both Stadis-450 and triethylamine in octane.

4.3. Experimental section

The details of the experimental apparatus are described in chapter three. Only deviations and specific implementations are presented.

4.3.1. Experimental conditions

Solvents *n*-heptane (99.5%, Mallinckrodt), *n*-octane (97% GC grade, Alfa-Aesar) and *p*-xylene (99+% HPLC grade, Aldrich) were used without further purification. The conductivity enhancer, Stadis-450 (Octel America), was added in 1% by volume to n-heptane and n-octane and 0.1% to *p*-xylene. The electrospray needle was held 2 mm away from the first aperture of the IMS and maintained at 875 V for n-heptane and n-octane, and maintained at 1060 V for p-xylene. In each case, solution flow rates were 0.2-0.5 μL min^{-1} and dry nitrogen gas flowed downward through the cell at 0.3 L min^{-1} or 0.6 cm s^{-1}.

	dielectric constant, ε	surface tension, γ (mN s^{-1})	percent charge loss	percent Rayleigh limit	evaporation temperature, T_d (K)	theor. slope, s (μm^2 s^{-1})	experim. slope, s (μm^2 s^{-1})
acetonitrile	36.64	28.66	15-20	100	270	-6500	n/a
methanol	33.0	22.07	15-20	120	267	-4750	n/a
water	74.6	71.99	20-40	100	278	-1250	n/a
n-heptane	1.921	19.65	19 (6)	101 (4)	278	-11900	-11000
n-octane	1.944	21.14	17 (10)	87 (8)	287	-3670	-4900
p-xylene	2.274	28.01	17 (6)	89 (3)	289	-2200	-2400

Table 4.1. Physical parameters and experimental charge loss values for solvents characterized by the "ping-pong" technique. Values in parenthesis are standard deviations. Acetonitrile, methanol and water data are taken from Smith and coworkers.[1] Physical constants at 293K are taken from Lide.[12] Theoretical evaporation parameters are calculated from equations in Chapter 3.

4.3.2. Electrospray ionization mass spectrometry

A Finnigan LCQ ion trap quadrupole mass spectrometer acquired the mass spectra. A custom built source using a fused-silica nanospray needle (New Objective, 15 μm I.D. tip) replaced the standard electrospray ion source. During acquisition, the capillary was not heated and the sheath gas was removed. The signal was optimized using the built-in tuning capabilities of the LCQ. Triethylamine (99.5%, Aldrich) was used without further purification.

4.4. Results

Representative data for a single droplet of *p*-xylene are shown in Figure 4.1. Large, simultaneous decreases in velocity and charge signal the occurrence of discharge events, as indicated by arrows. Specifically, plot (a) shows constant evaporation and a steadily decreasing diameter. Initially, constant charge and decreasing mass leads to an increase in the velocity (b) as the electric force, qE, steadily becomes stronger relative to the force of gravity, m_pg. The small oscillations in velocity correspond to motion with and against gravity. As a result of constant charge (c) and steadily decreasing mass, the droplet approaches its Rayleigh limit (d). This trend continues for the first 0.14 s of the droplet data acquisition at which point the velocity, charge, and percent Rayleigh limit ($100q\ q_R^{-1}$) decrease dramatically. The sudden decrease in droplet charge results in a similarly large decrease in velocity, as the change in qE is significantly larger than the change in m_pg. We interpret this rapid loss of charge to be a Rayleigh discharge event.

Table 4.1 summarizes the discharge and evaporation characteristics of the three solvents studied along with the corresponding data for acetonitrile, water and methanol

previously reported from our laboratory.[1]   Between discharge events, individual charge

values are averaged, which is illustrated by the dotted lines in Figure 4.1(c).   Percent

charge loss is determined from the difference between the average charge levels before

and after a discharge event.   The percent Rayleigh limit at discharge is simply the last

recorded value before the sharp decrease characteristic of a discharge event.   Both the

percent charge lost and the percent Rayleigh limit data are explored with histograms for

each solvent in Figure 4.2(a) and (b), respectively.   As the distribution of each is roughly

Gaussian in shape, Table 4.1 lists standard deviations for these data in parentheses.   A

linear regression of diameter squared versus time generates the parameters that quantify

evaporation.   Figure 4.3 shows an example of the fitting performed on the diameter

measurements from Figure 4.1(a).   The resulting slope values are averaged in Table 4.1

for each solvent.   Note that this treatment ignores diameter decreases that result from

discharge events.

Both *n*-octane and *p*-xylene were often characterized through 30-50 reversals of

the electric field.   Up to seven discharge events were observed for n-octane, while p-

xylene demonstrated up to eight.   For example, the acquisition shown in Figure 4.1

contains five well-defined discharge events highlighted by arrows.   Heptane rarely

exhibited multiple discharges because its higher evaporation rate results in a shorter

residence time in the IMS.   Size-charge correlations for droplets from these solvents are

shown together in Figure 4.4.   The data represent the diameter versus charge for each

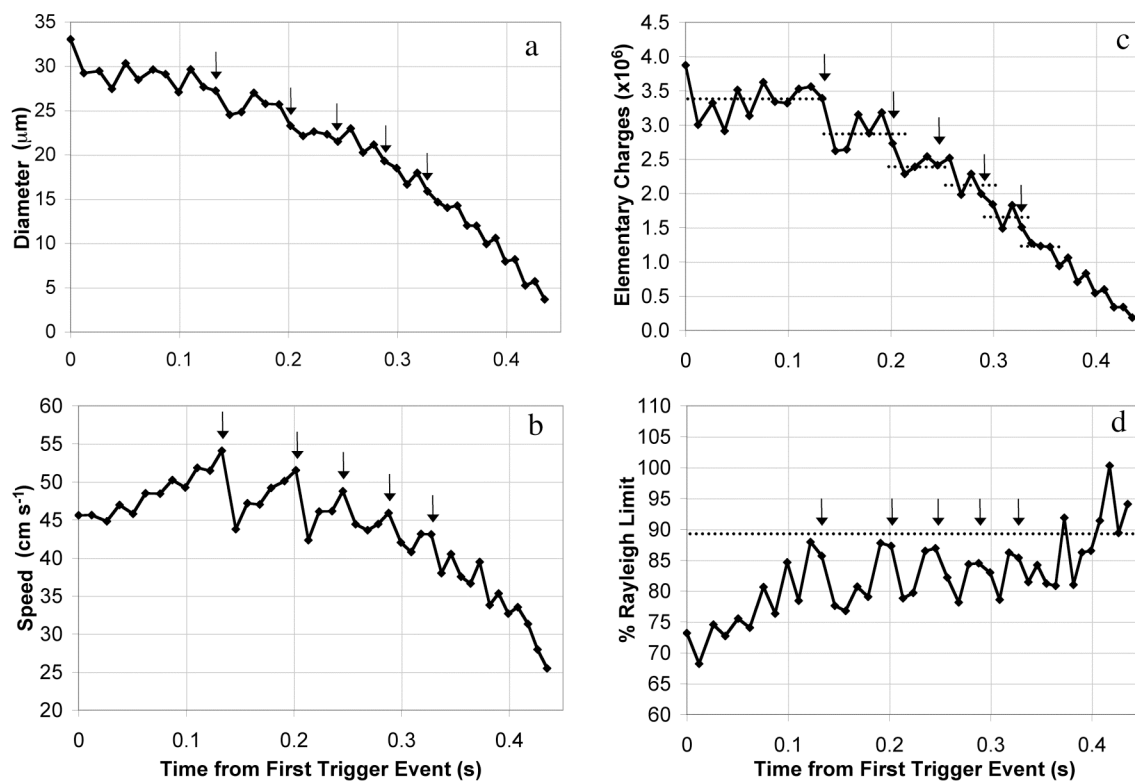droplet immediately preceding its first recorded discharge event.

Figure 4.1. Acquired history of a droplet of *p*-xylene including (a) size, (b) velocity, (c) charge, (d) percent Rayleigh limit. As the droplet evaporates its speed increases and charge stays constant until it discharges. Discharge events (indicated by arrows) occur at approximately 90% the Rayleigh limit and are characterized by charge loss of approximately 20% and undetectable mass loss.
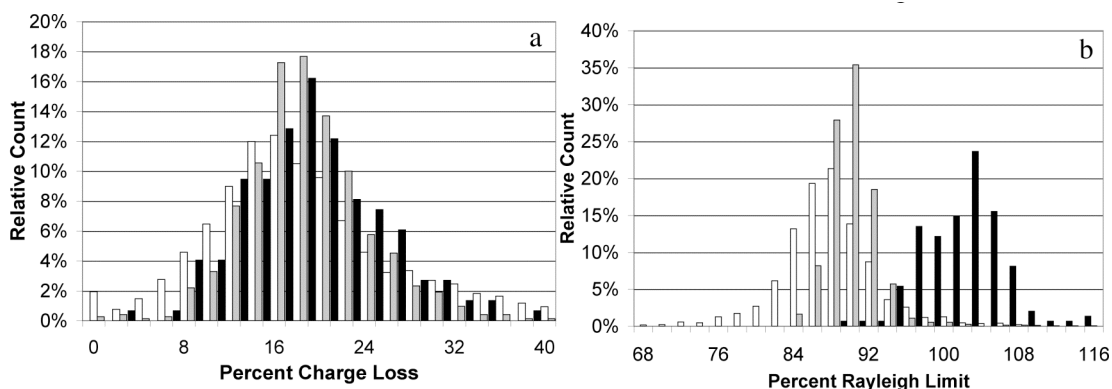
Figure 4.2. Histograms of (a) percent charge lost and (b) percent Rayleigh limit at the point of discharge for each observed discharge event. Due to unequal sample sizes, each histogram is reported as a fraction of the total for each respective solvent. In both histograms, black bars represent n-heptane, white bars represent *n*-octane, and gray bars represent *p*-xylene.
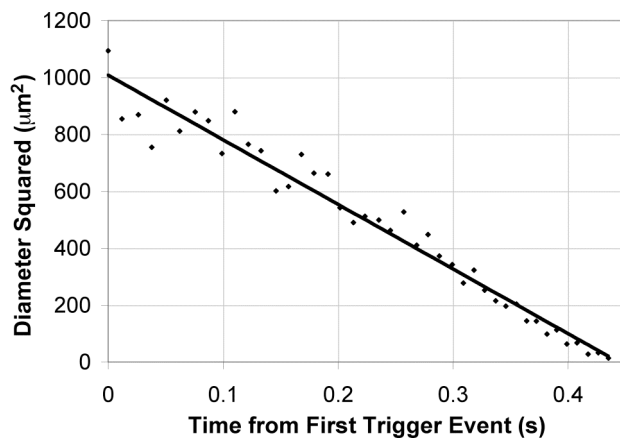

Figure 4.3. Diameter squared versus time for the acquisition shown in Figure 4.1. A linear regression analysis yields a slope $s = -2271\ \mu m^2\,s^{-1}$ that characterizes solvent evaporation. Average experimental values for the slopes of all three solvents are presented in Table 4.1.
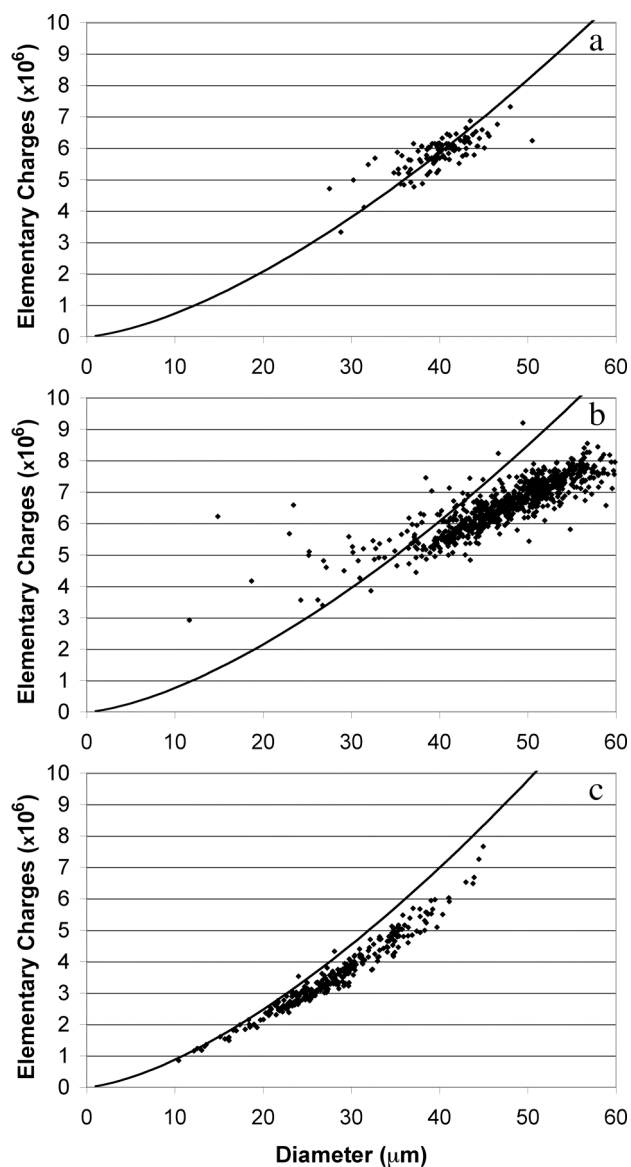
Figure 4.4. Size-charge correlation diagrams for (a) *n*-heptane, (b) *n*-octane, and (c) *p*-xylene for all droplets immediately preceding the first recorded discharge event. Solid lines show the Rayleigh limit for each solvent. The droplet size-charge correlations for heptane and octane are tightly clustered, indicating monodisperse droplet formation for these solvents. In contrast, *p*-xylene droplets are observed over a wide range of size and charge.
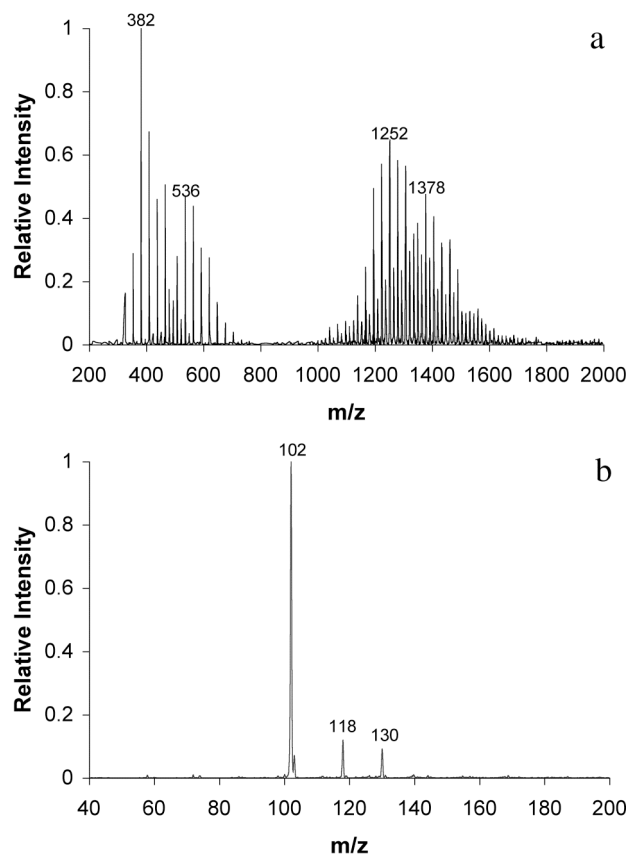
Figure 4.5. Mass spectra of (a) Stadis-450 and (b) triethylamine in octane. Stadis-450 is characterized by two pairs of overlapping distributions centered on 382, 536, 1252, and 1378 m/z. Peaks are separated by 28 m/z units within each distribution are indicative of a hydrocarbon polymer. The protonated triethylamine spectrum (b) shows contaminants at 118 and 130 m/z.

Figure 4.5 shows two mass spectra using n-octane as the electrospray solvent. Spectrum (a) is the averaged mass spectrum showing that a complex array of ions is present when Stadis-450 is added to *n*-octane. Spectrum (b) exhibits the ions observed when triethylamine is added to neat *n*-octane.

4.5. Discussion

4.5.1. Size-charge distributions

Plots in Figure 4.4 show typical diameters of 35-45 μm for heptane (a), 35-60 μm for octane (b), and 10-40 μm for *p*-xylene (c). The droplets in the present study are larger than those produced by common nanospray techniques, but are comparable to the sizes employed in other studies of Rayleigh discharge.[9,13,14] In plotting points immediately preceding the first recorded discharge event for each droplet, Figure 4.4 explores the point at which droplets discharge relative to the Rayleigh limit. Size-charge distributions for latter discharge events resemble those shown in Figure 4.4 and show no additional patterns of interest. Size versus charge does not scale with the Rayleigh limit curves for either heptane or octane as shown on plots (a) and (b), respectively. In both cases, smaller droplets discharge at a higher percent Rayleigh limit than the larger droplets studied. In contrast, *p*-xylene discharges scale with the Rayleigh limit over the size range studied. The distributions in Figure 4.4 support the broader standard deviation in the percent Rayleigh limit at the point of discharge for n-octane and the smaller deviation for *n*-heptane and *p*-xylene listed in Table 4.1 and shown by the histograms in Figure 4.2.

4.5.2. Evaporation and discharge dynamics

The average charge loss in a discharge event for all three solvents is $18 \pm 1\%$. This corresponds favorably with studies by Taflin and coworkers, who reported highly accurate measurements on twelve discharge events of low-volatility oils.[13] Our data for over two thousand discharge events indicate that similar charge loss is observed for high-volatility hydrocarbon solvents as well.

Droplet diameter decreases in time due to solvent evaporation, as is evident in Figure 4.1. Within the accuracy of the measurements, no observable discrete decrease in diameter accompanies the discharge events indicated by arrows. The 4% experimental error in our diameter measurement is significantly larger than that of Taflin and coworkers who report droplet radii between 10-20 μm to within 1 nm.[13] Their observed 2% mass loss would correspond to a 0.7% change in diameter which is significantly below the resolution of our PDA. Therefore we are only able to put an upper bound on the change in diameter at 4%, corresponding to the experimental error in our measurements.

4.5.3. Successive discharges

Earlier "ping-pong" studies in our lab revealed up to five discharge events from a single parent droplet in experiments with methanol.[1] The electric field generated in the IMS is radially uniform and time-independent transverse to droplet motion along the axis of the instrument. This method contrasts with electrodynamic balance experiments, which suspend individual droplets with time-dependent axial and radial fields.[15] To observe multiple discharge events from the same droplet in the IMS, the droplet must not drift

radially beyond the 150 μm diameter of the PDA measurement volume. Radial momentum is either a result of a droplet's original path, or from another force imparted on it during its residence time in the IMS. The observation of multiple discharges implies that the net position of the droplet is not significantly affected by a discharge event. On this assumption, Smith discusses the implications for the maximum impulse imparted to the parent droplet.[2] However, recent observations from Leisner and coworkers of simultaneous emission of two progeny droplet streams in opposite directions would be expected to impart little, if any, momentum to the parent droplet.[10]

The decreasing time between successive discharges is consistent with the theoretical treatment by Tang and Smith in which the time between discharges is a function of droplet diameter.[16] Indeed, since q_R is proportional to $r^{3/2}$ according to the Rayleigh limit equation $q_R = 8\pi\varepsilon^{1/2}\sigma^{1/2}r^{3/2}$ and r^2 decreases linearly in time from evaporation, it comes as no surprise that the time between events is decreasing. Beyond the five discharges in Figure 4.1, events occur faster than the 100 Hz data acquisition rate of the experiment. This leads to the observed steady decrease in velocity, as well as the unreliable charge and percent Rayleigh limit information evident in the later period of the acquisition. Further analysis of the multiple discharges in *n*-octane and *p*-xylene reveal that within experimental error, there is no change in the percent charge lost in successive discharge events.

4.5.4. Comparison of discharge characteristics with polar solvents

The data in Table 4.1 for the six solvents studied with the "ping-pong" experiment suggest a correlation between the percent charge lost and both the dielectric constant, ε,

and the surface tension, γ, of the solvent. This compares favorably with Fernandez de la

Mora's predictions for charge and solvent flow through a discharge event.[17] We assume

the electrical conductivity of 4.1 x 10^{-8} S cm^{-1} measured by Tang and Gomez for 1.2%

Stadis-450 in *n*-heptane represents a maximum conductivity for the solutions in the

present study.   Consequently, there is no correspondence between the discharge

characteristics and solution conductivity, which would be significantly higher for the

methanol solutions. Previous work in our lab found no significant change in the percent

charge lost in a discharge event in methanol solutions with varying concentrations of

sodium chloride.[1] This suggests percent charge loss is also dependent on factors not yet

explored.

4.5.5. Application to electrospray mass spectrometry

While enhancing the conductivity, Stadis-450 is not a desirable additive for

electrospray ionization using hydrocarbon solvents.   Figure 4.5(a) shows the mass

spectrum of Stadis-450 (1% by volume) in octane. The complex distribution illustrated

may be difficult to separate from that of an analyte. The spectrum of Stadis-450 is

characterized by two pairs of overlapping distributions with peaks separated by 28 m/z

indicating the presence of a polymer with a distribution of polymer chain lengths.

Triethylamine was sprayed in octane in a separate experiment without the Statis-450

additive. In positive ion mode, protonated triethylamine appears at 102 m/z. The process

leading to protonation of the amine in octane was not investigated, and may have

involved trace impurities as the charge carriers in the droplet.

4.6. Conclusions

Heptane, octane, and *p*-xylene have discharge characteristics similar to those found for both large, low-volatility hydrocarbons and for traditional electrospray solvents. Successive discharge events observed for *n*-octane and *p*-xylene demonstrate no significant change in the percent charge lost for both *n*-octane and *p*-xylene. Size-charge correlations for heptane and octane show that smaller droplets discharge at a higher percent Rayleigh limit of charge than larger droplets. Over the size range studied, *p*-xylene discharges at a consistent charge relative to its Rayleigh limit.

The combination of appropriate conductivity and evaporation rates make these solvents attractive for electrospray mass spectrometry. The introduction of these hydrocarbon solvents may be important for mass spectrometry applications for analytes that do not dissolve easily in other solvents, or those already dissolved in a hydrocarbon solvent and not easily extracted into a more traditional electrospray environment. With a complicated spectrum, Stadis-450 is not an appropriate conductivity enhancing agent as it could interfere with the interpretation of analyte spectra.

4.7. Acknowledgements

4.8. References

(1)   Smith, J. N.; Flagan, R. C.; Beauchamp, J. L. *J. Phys. Chem. A* **2002**, *106*, 9957.

(2)   Smith, J. N. Fundamental Studies of Droplet Evaporation and Discharge Dynamics in Electrospray Ionization, California Institute of Technology, 2000.

(3)   Zhan, D.; Fenn, J. B. *Int. J. Mass Spectrom.* **2000**, *194*, 197.

(4)   Hughey, C. A.; Rodgers, R. P.; Marshall, A. G. *Anal. Chem.* **2002**, *74*, 4145.

(5)   Roussis, S. G.; Proulx, R. *Anal. Chem.* **2002**, *74*, 1408.

(6)   Schalley, C. A.; Rivera, J. M.; Martin, T.; Santamaria, J.; Siuzdak, G.; Rebek, J. *Eur. J. Org. Chem.* **1999**, *6*, 1325.

(7)   Hof, F.; Rebek, J., Scripps Research Institute, La Jolla, CA. Personal communication regarding the use of xylene as an electrospray solvent, 2001.

(8)   Tang, K.; Gomez, A. *J. Colloid Interface Sci.* **1996**, *184*, 500.

(9)   Gomez, A.; Tang, K. *Phys. Fluids* **1994**, *6*, 404.

(10)   Duft, D.; Atchtzehn, T.; Muller, R.; Huber, B. A.; Leisner, T. *Nature* **2003**, *421*, 6919.

(11)   Hager, D. B.; Dovichi, N. J.; Klassen, J.; Kebarle, P. *Anal. Chem.* **1994**, *66*, 3944.

(12)   *CRC Handbook of Chemistry and Physics*; 76th ed.; Lide, D. R., Ed.; CRC Press: Boca Raton, FL, 1995.

(13)   Taflin, D. C.; Ward, T. L.; Davis, E. J. *Langmuir* **1989**, *5*, 376.

(14)   Davis, E. J.; Bridges, M. A. *J. Aerosol Sci.* **1994**, *25*, 1179.

(15)   Davis, E. J. *Aerosol Science and Technology* **1997**, *26*, 212.

(16)   Tang, K.; Smith, R. D. *International Journal of Mass Spectrometry* **1999**, *185/186/187*, 97.

(17)   Fernandez de la Mora, J. *J. Colloid and Interface Sci.* **1996**, *178*, 209.